Nuclear Instruments and Methods in Physics Research A 363 (1995) 124–127

ELSEVIER

NUCLEAR INSTRUMENTS & METHODS IN PHYSICS RESEARCH Section A

Accurate and fast computation of high order fringe-field maps via symplectic scaling

Georg Heinz Hoffstätter *, Martin Berz [1]

Department of Physics and Astronomy and National Superconducting Cyclotron Laboratory, Michigan State University, East Lansing, MI 48824, USA

Abstract

The fringe fields of particle optical elements often have a significant influence on particle motion, particularly on the higher order aberrations of instruments. Using DA methods, it is possible to compute high order transfer maps of the fringe-field region exactly by integration, but compared to the determination of the main field effects, the method is rather time consuming. Here we introduce an approximate calculation scheme which is very accurate and fast and is therefore particularly useful for efficient optimization of field parameters. It works to arbitrary order and yields order by order symplectic Taylor maps. With this method, the speed of computing fringe-field maps is typically increased by up to two orders of magnitude.

1. Introduction

Using propagation operators, the Differential Algebraic (DA) methods [1,2] allow very fast computation of high order maps of the main-field region of particle optical elements. High order transfer maps of the fringe-field region, however, can only be calculated accurately using rather time consuming numerical integration in DA [1–3]. Typically, such integration is up to three orders of magnitude slower than the evaluation of the propagator. Since in many cases fringe-field effects of optical elements dominate aberration coefficients, the effort for their calculation thus limits the speed of calculations.

It is therefore desirable to develop methods for accurate and fast approximation of the effects of fringe-field maps. The methods should work to arbitrary order and preserve the relationships between the matrix elements imposed by the symplectic symmetry. Furthermore, it should work for any type of instrument to allow application in all the various subfields of particle optics.

In the past, a variety of fast approximations have been used. However, all of them have some undesirable features which should be circumvented. The mere neglect of fringe-field effects, often referred to as Sharp Cut Of Fringe Field (SCOFF) approximation, is very inaccurate. Low accuracy numerical integration is not accurate and not symplectic. The impulse approximation used in TRANSPORT [4,5] only considers the first and the second order and is only applicable for small apertures. Fringe-field integral methods, which are employed in the code GIOS [6] cannot be used for solenoids and large aperture instruments, and the obtained maps are in general not symplectic. Furthermore, the method is so far only available to third order, although attempts are being made to extend it to fifth order for some cases [7].

We introduce a method which does not have these drawbacks. It is particularly suited for the optimization process since the speed and accuracy are most advantageous when fringe-field maps are computed repeatedly with slightly different parameters. This mode of computing fringe-field maps has been implemented in the arbitrary order code COSY INFINITY [2,8], which was used for the computation of all the examples provided in this paper.

2. Outline of the principles

A detailed description of the principle of symplectic scaling, which forms the basis of the method for the fringe field approximation, is given in Ref. [3]. It is not within the scope of this paper to describe the relevant nonlinear transformations in detail or to dwell on the different systems of coordinates which have to be used. Therefore we will restrict ourselves to a brief discussion of the key ideas of symplectic scaling and then demonstrate its usefulness and its accuracy in several practical cases.

* Corresponding author. Now at DESY, 22603, Hamburg, Germany. E-mail hoff@desy.de.

[1] Supported in part by the National Science Foundation, Grant Number PHY 89-13815, and the Alfred P. Sloan Foundation.

SSDI 0168-9002(95)00366-5

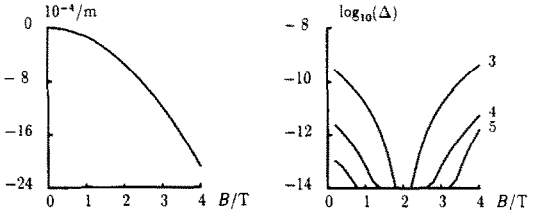

Fig. 1. Left: the matrix element $(x \mid xxa)$ for a quadrupole as a function of the field at the pole tip. Right: error Δ of the approximation of $(x \mid xxa)$ for various expansion orders of the reference representation at $B = 2$ T.

The symplectic scaling (SYSCA) approximation is based on two rather obvious scaling properties that are satisfied by maps of magnetic particle optical elements written in geometric coordinates $\boldsymbol{x} = (x, x', y, y', \delta_l, \delta_p)$, which are for example used in TRANSPORT. These are connected to the fact that the maps depend only on the ratio of field strength to magnetic rigidity on the one hand and on the product of field strength and the size of the element on the other hand.

Thus, once the map of an element is known for a given type of beam particle P as a function of the magnetic field strength at the pole tip, the first scaling property can be used to compute the map for any particle type P*, since the trajectory of P* is equivalent to the trajectory of P at a different magnetic field. With the second scaling property, the map can be computed for any similar element which is scaled in size, since the trajectory of a particle is only magnified by a scaling factor, if the size of the element is magnified and the strength of the field is demagnified by the same factor.

With these two scaling properties, the map of an optical element of any size and for any particle can be computed once the field dependence of the map for one given size and one particle type is known. While usually the map is not known as a function of the magnetic field, DA based programs can be used to approximate this functional dependence by Taylor expansion in a straightforward way.

For theoretical reasons, the resulting approximation can be expected to be very accurate. Applying perturbation theory to the problem, which is the basis of the fringe-field integral method [9–11], shows that the effects of the fringe fields depend on the field in a polynomial fashion, where higher order terms arise in higher order perturbation theory. Since the deviations from the unperturbed orbits are small and hence perturbation theory will converge quickly, these higher order contributions become less and less significant. This phenomenon will become apparent in practice in various examples given in the next sections.

In order to preserve the symplectic symmetry of the map, it is necessary to utilize symplectic representations. This assures that even after Taylor expansion in the field, while not being exact, the resulting map is still symplectic.

For reasons of speed, it proved advantageous to represent the linear part of the map by a generating function and the nonlinear part by a single Lie exponent. The generating function as well as the Lie exponent depend nonlinearly on the magnetic field. Now it is possible to scale not the field dependent map, but rather its field dependent symplectic representation. This leads to an approximate scaled symplectic representation representing an approximated scaled map which is guaranteed to be symplectic. The field dependent symplectic representation, saved in a reference file, is the basis for computing maps via symplectic scaling.

3. Fringe-field maps

Traditionally, the main-field region and the fringe-field region are separated since the autonomous equations of motion in the main-field region can be solved much easier than the non-autonomous ones in the fringe-field region. In order to describe the difference between the transfer map of an optical instrument and the transfer map given by only its main-field region, each optical element is sandwiched between so-called entrance and exit fringe-field maps that describe the effects attributable to fringe fields only.

The maps of the drift and of the main-field region can be computed quickly by explicit formulas and by evaluating the propagation operator. The computation of the fringe-field maps on the other hand is performed by symplectic scaling.

To illustrate the practical use and accuracy of this method, we compute the third order matrix element (x, xxa) of a quadrupole with fringe fields in two ways,

Table 1

Angle	(a, xa)		(x, xaa)	
	SYSCA	DA integration	SYSCA	DA integration
5°	−0.1360314E − 02	−0.1368305E − 02	−0.6524050E − 01	−0.6520405E − 01
10°	−0.7231982E − 03	−0.7253955E − 03	0.5269389E − 03	0.5795750E − 03
15°	−0.1033785E − 06	−0.2891228E − 08	0.7179696E − 01	0.7179678E − 01
20°	−0.1718367E − 02	−0.1721275E − 02	0.1463239	0.1461203
25°	−0.9628906E − 02	−0.9643736E − 02	0.2187553	0.2180152
30°	−0.2977263E − 01	−0.2981580E − 01	0.2775432	0.2755090

Table 2

B_H/T	(a, xa)		(x, aaa)	
	SYSCA	DA integration	SYSCA	DA integration
0.0	0.00000	0.00000	0.0109946	0.0109946
0.1	−2.54411	−2.54412	0.0400742	0.0400755
0.2	−5.08823	−5.08824	0.1273131	0.1273182
0.3	−7.63235	−7.63236	0.2727113	0.2727228
0.4	−10.17647	−10.17649	0.4762688	0.4762891
0.5	−12.72058	−12.72061	0.7379855	0.7380173

namely by DA integration of the non-autonomous equations of motion, and by sandwiching the main-field map into the entrance and exit fringe-field maps obtained by symplectic scaling. Fig. 1 shows the dependence of the matrix element as a function of field strength as well as the accuracy of the SYSCA method for various orders of the expansion in field strength. As can be observed, depending on the order, the accuracy lies in the range of nine to thirteen digits, even if the field strength deviates by a factor of two from the reference field strength.

4. Edge angles and edge curvatures

In practice, bending magnets often employ edge angles as well as edge curvatures to achieve focusing or to influence nonlinear matrix elements. In order to avoid the computation of a reference file for different edge angles and curvatures, in the practical use of the SYSCA method, a further approximation is used. The effect of the edge shape is evaluated by first applying the fringe-field map of a straight edge dipole, and then taking edge angles and curvatures up to second order into account analytically in the main field of the elements. Higher order curvatures are treated in a kick approximation. In this way, edge effects and effects depending on finite size are decoupled, which is expected to work accurately as long as the perturbations due to the finite size of the fringe field are small.

Table 1 demonstrates the practical accuracy of this approximation. In our example, we used a dipole of radius 2 m, a bend angle of 30°, and an aperture of 1 in. The Taylor coefficients (a, xa) and (x, xaa) were computed with SYSCA (left) and with accurate numerical integration in DA (right) for different edge angles. In all examples, the entrance and the exit edge angle are equal.

5. SYSCA for superimposed multipoles

The computation of the effect of the fringe field of superimposed multipoles can be achieved in a similar way as in the case of edge angles and curvatures. The total effect is approximated by applying the individual multipole fringe-field maps sequentially. While appearing crude, because of the perturbative nature of the various fringe-field maps, the method actually gives very accurate results. In Table 2, SYSCA (left) and exact DA integration (right) were used to compute coefficients of the fringe-field map of a magnetic quadrupole which is superimposed with a magnetic hexapole. The device has an aperture of 1 in. and is 0.5 m long. The pole-tip field of the quadrupole was 1 T and the pole tip-field B_H of the hexapole is given in Table 2.

6. Approximating maps of solenoids with SYSCA

While primarily geared towards the entrance and exit fringe fields of particle optical elements, the SYSCA method can also be used in cases where these fringe fields overlap. A typical example is the magnetic solenoid, in which the fringe fields even provide the focusing properties, and which otherwise can only be treated by DA integration. In this case it is advantageous to not perform a separation into parts, but to treat the whole element in one piece.

In Table 3 the focal length and the third order opening aberration of a solenoid is shown, calculated both by exact DA integration and by using the SYSCA method. Apparently, SYSCA is reliable over a wide range of focal lengths. The solenoid used has a length of 6 mm and an aperture of 4 mm, and B_H is the field in the center.

7. Spectrograph calculations

In this section, we illustrate the use of the method for a practical high-order calculation using the high-resolution large-acceptance spectrograph S800 and its dispersion

Table 3

B_H/T	f mm		(x, aaa) mm	
0.10	168.3905	168.4225	2.711050	2.713369
0.15	75.6999	75.6974	2.363293	2.363727
0.20	43.2568	43.2555	1.890587	1.890608
0.25	28.2534	28.2529	1.310832	1.310838
0.30	20.1181	20.1180	0.646378	0.646473
0.35	15.2287	15.2288	−0.076121	−0.075216
0.40	12.0723	12.0729	−0.825480	−0.822073

matching beamline, which are under construction at NSCL. We begin by performing an adjustment of the operating parameters of the device using the code COSY, which requires fitting of 14 linear and 6 second order conditions. This was done using different computation methods for the fringe fields; as is apparent, the SYSCA method provides a dramatic improvement in computation speed: only main fields with propagator: 51 s; fringe fields with DA integration: 7 h 11 min; fringe fields with SYSCA: 6 min 38 s.

As a second example, we study the A1200 isotope separator [12] at NSCL. Linear and nonlinear effects are analysed to demonstrate on the one hand the necessity of taking fringe fields into account and on the other hand the accuracy which is achieved with SYSCA.

To show the effect of fringe fields to first order, we compare quadrupole settings which satisfy the first order conditions of the beamline for different fringe-field maps. The fringe fields were described by Enge functions, and the Enge coefficients have been fitted to measured field data. The CPU time used for the fit was 3 min for SYSCA versus two hours for numerical integration in DA.

To demonstrate SYSCA's accuracy for nonlinear effects, we study the tilt angle Θ of the dispersive image plane and the opening aberration C_O. In the discussed device the coefficient $(x \mid aa)$ vanishes because of symmetry of the axial ray and anti-symmetry of the dipole fields; therefore $(x \mid aaa)$ is the relevant opening aberration,

$$\Theta = -\frac{(x \mid a\delta)}{(a \mid a)(x \mid \delta)}, \quad C_O = (x \mid aaa).$$

Table 4 shows Θ and C_O for various fringe-field models. The third order aberration is totally inaccurate if fringe fields are disregarded. This table also shows that quadrupole fringe fields, although often disregarded, can have effects which dominate over dipole fringe fields.

Table 4

Θ and C_O with SCOFF approximation	80.8840°	−65.96 m
Θ and C_O with dipole fringe fields only	81.1696°	−65.96 m
Θ and C_O with quad fringe fields only	81.2694°	−682.68 m
Θ and C_O with SYSCA approximation	81.2701°	−687.10 m
Θ and C_O with actual fringe fields	81.2702°	−687.10 m

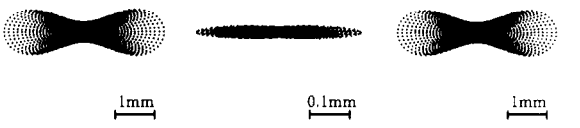

Fig. 2. Beam spots obtained with the exact map (left), with TRANSPORT approximation (middle) and with SYSCA approximation (right). Notice the difference in scale.

The combined effect of several nonlinear coefficients can be seen by sending a cone of particles through the seventh order map of the A1200. The images with SCOFF and SYSCA approximation as well as the exact calculation are shown in Fig. 2. The maximum angle used is 15 mrad. Note that due to the difference in scale, the beam spot computed with SCOFF is only one tenth as big. Trusting SCOFF would lead to a loss of most of the beam.

References

[1] M. Berz, Nucl. Instr. and Meth. A 298 (1990) 426.
[2] M. Bertz, these Proceedings (4th Int. Conf. on Charged Particle Optics, Tsukuba, Japan, 1994) Nucl. Instr. and Meth. A 363 (1995) 100.
[3] G.H. Hoffstätter, Rigorous bounds on survival times in circular accelerators and efficient computation of fringe-field transfer maps, Ph.D. thesis, Michigan State University, East Lansing, MI 48824, USA p (1994).
[4] K.L. Brown, F. Rothacker, D.C. Carey and Ch. Iselin, TRANSPORT user's manual, Technical Report SLAC-91, Stanford Linear Accelerator Center (1977).
[5] R.H. Helm, First and second order beam optics of a curved inclined magnetic field boundary in the impulse approximation, Technical Report 24, SLAC (1963).
[6] B. Hartmann, M. Berz and H. Wollnik, Nucl. Instr. and Meth. A 297 (1990) 343.
[7] B. Hartmann, H. Irnich and H. Wollnik, in: Nonlinear Problems in Accelerator Physics, Conf. Ser. No. 131 (Institute of Physics, London, 1993) p. 87.
[8] M. Berz, COSY INFINITY version 6 reference manual, Technical Report MSUCL-869, National Superconducting Cyclotron Laboratory, MSU, East Lansing, MI (1992).
[9] K.L. Brown, R. Belbeoch and P. Bounin, Rev. Sci. Instr. 177 (1964) 481.
[10] H. Wollnik, Nucl. Instr. and Meth. (1965) 38.
[11] H. Rose, Nucl. Instr. and Meth. A 258 (1987) 374.
[12] B.M. Sherrill, Nucl. Instr. and Meth. B 70 (1992) 298.